

Sensitivity of jet quenching to the initial state in heavy-ion collisions

Souvik Priyam Adhya^{✉*}

*Institute of Physics of the Czech Academy of Sciences,
Na Slovance 1999/2, 18221 Prague 8, Czech Republic and
Institute of Nuclear Physics, Polish Academy of Sciences, ul. Radzikowskiego 152, 31-342 Krakow, Poland*

Konrad Tywoniuk[†]

*Department of Physics and Technology, University of Bergen, 5007 Bergen, Norway
(Dated: September 9, 2024)*

In heavy-ion collisions, nuclear matter is subjected to extreme conditions in a highly dynamical, rapidly evolving environment. This poses a tremendous challenge for calculating jet quenching observables. Current approaches rely on analytical results for static cases, introducing theoretical uncertainties and biases in our understanding of the pre-equilibrated medium. To address this issue, we employ resummation schemes to derive analytical rates for radiative energy loss in generic, evolving backgrounds. We investigate regimes where rare scattering and multiple scattering with the dynamical medium occurs, and extract relevant scales governing the in-medium emission rate of soft gluons. Our analysis indicates that strong jet quenching is only possible when the equilibration time of the medium is longer than its mean free path, highlighting the importance of medium modifications of jets in the earliest stages of heavy-ion collisions. We also demonstrate analytically that a medium evolution, which initially has a small coupling to jets, typically leads to a stronger jet azimuthal asymmetry at the same jet suppression factor.

PACS numbers: 12.38.-t, 24.85.+p, 25.75.-q

Introduction: The quark-gluon plasma (QGP), created in relativistic heavy-ion collisions, is short-lived but leaves a strong imprint on particle production. The focus of this work is on the high-energy particles that pass through the QGP and can be used to study its microscopic properties. These particles are detected as collimated sprays of particles and energy, called jets [1, 2]. Jet modifications [3–8], compared to a baseline obtained in proton-proton collisions, have been studied extensively for over a decade at RHIC and LHC [9–31]. The magnitude of these modifications is quantified by the suppression factor, R_{AA} , which is the ratio of the jet yield in heavy ion collisions to that in proton-proton collisions scaled by the number of binary nucleon-nucleon collisions, and the dependence on medium geometry is probed through the azimuthal flow harmonic coefficient v_2 of jets. In addition, other jet observables, such as jet shapes, fragmentation patterns, and substructure measurements, have also been studied [32–36]. These observables provide complementary information on the phenomenon of jet quenching to investigate the properties of the QGP.

The produced jets are moving through a constantly evolving and diluting background. Jet quenching observables therefore capture both the integrated and differential properties of medium evolution, making them sensitive to various stages of heavy-ion collisions. At late times, the bulk matter achieves a state of “hydrodynamic” equilibrium, meaning that its subsequent evolution can be captured by nearly-perfect hydrodynamics [37]. In the Bjorken model [38], representing

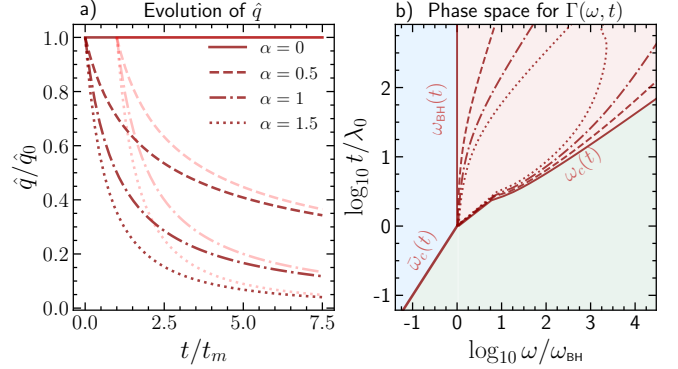


FIG. 1: a) Two models for the evolution of \hat{q} , model (i) represents the equilibration of an initially over-occupied system, while (ii) corresponds to an initially under-occupied system. b) Evolution of the relevant energy scales governing the in-medium emission rate $\Gamma(\omega, t)$.

boost-invariant relativistic hydrodynamics, the QGP energy density ε evolves according to $\varepsilon(t) = \varepsilon_0(t_0/t)^{1+c_s^2}$, where ε_0 is the initial energy density, t_0 is the initial time of the hydrodynamical evolution and $c_s^2 = \partial P/\partial \varepsilon$ is the speed of sound. In an ideal, relativistic plasma, $c_s^2 = 1/3$. Since the jet transport parameter behaves like $\hat{q} \propto g^4 \varepsilon^{3/4} \sim t^{-1}$, describing both the momentum broadening of propagating particles and governs energy loss in the medium, we should expect that the jet quenching effects gradually weaken during the hydrodynamic expansion of the QGP [39–42]. In this work, we consider a class of generalized models with $\hat{q} \sim t^{-\alpha}$, see Fig. 1a).

* adhya@fzu.cz

† konrad.tywoniuk@uib.no

How the hot and dense medium evolves prior to the equilibration time is largely an open question. For an initially over-occupied system of gluons one expects the so-called “bottom-up” equilibration scenario [43–47] that indicates a rapid growth of the momentum broadening of hard partons followed by a gradual decay [48–53]. As an illustrative example [50], $\hat{q} \approx 6 \text{ GeV}^2/\text{fm}$ at the very early stages of the collision $\tau \sim 0.06 \text{ fm}$ [54]. In contrast, when starting in an under-occupied partonic system there is a certain delay before interactions overcome the rapid longitudinal expansion of the system, causing \hat{q} initially to grow before reaching a maximum value, subsequently followed by a hydrodynamic decay.

In this work, we assess the potential of jet quenching observables to capture the imprint of early dynamics in heavy-ion collisions. To accomplish this, we propose two distinct scenarios. Model (i) aims at capturing the characteristics of an initially over-occupied system, featuring an initial large value of \hat{q} with a subsequent decay. In contrast, model (ii) allows for a delayed onset of quenching effects up to a thermalization time t_m . To allow for flexibility, t_m is independent of the mean free path of elastic scattering λ . In both cases we consider a flexible parameterization of the hydro-like regime, $\hat{q} \sim t^{-\alpha}$, see Fig. 1a) for details.

In order to tackle these questions, we first derive analytical in-medium emission rates to calculate energy loss that are valid for any medium expansion scenario. This can be achieved by using established schemes to deal with scattering on a background medium [55], including the IOE approach [56–60]. While earlier studies assumed a static medium, this letter extends the analysis to include the relevant energy scales that govern radiative energy loss in an expanding medium. This allows us to determine the validity of the multiple, soft and rare, hard scatterings not only as a function of energy but also as a function of the initial quenching time of the medium, see Fig. 1b). This novel approach allows us to determine whether multiple scatterings play a significant role in dynamical systems, which in turn influences the design of radiative in-medium parton showers.

Theoretical formalism. We study the medium-induced spectrum for emitting soft gluons, $\Gamma(\omega, t) = dI^{\text{med}}/(d\omega dt)$ [61–63], which reads [55, 64]

$$\Gamma = \frac{4\alpha_s C_R}{\omega^2} \int_0^t dt_0 \int_{\mathbf{p}, \mathbf{p}_0} \Sigma(\mathbf{p}^2, t) \frac{\mathbf{p} \cdot \mathbf{p}_0}{\mathbf{p}^2} \tilde{\mathcal{K}}(\mathbf{p}, t; \mathbf{p}_0, t_0), \quad (1)$$

where C_R is the color charge of the emitting particle and $\Sigma(\mathbf{p}^2, t) = \int_{\mathbf{q}} \Theta(\mathbf{q}^2 - \mathbf{p}^2) \sigma(\mathbf{q}, t)$, with the scattering potential off gluons in the medium being encoded in $\sigma(\mathbf{q}, t) = N_c n(t) d\sigma_{\text{el}}/d^2\mathbf{q}$ [65]. Here, where $n(t)$ denotes the density of scattering centers. Finally, with $\tilde{\mathcal{K}} = (-\text{Im})\mathcal{K}$, the three-point correlator $\mathcal{K}(\mathbf{p}; \mathbf{p}_0)$ describes the transverse momentum broadening experienced by the gluon during its formation time, and is the Green’s function of a Schrödinger equation in transverse-coordinate space, i.e. $[i\partial_t + \partial_{\perp}^2/(2\omega) + iv(\mathbf{x}, t)]\mathcal{K}(\mathbf{x}, t; \mathbf{y}, t_0) =$

$i\delta(\mathbf{x} - \mathbf{y})\delta(t - t_0)$, where the time-dependent medium potential $v(\mathbf{x}, t)$ is related to the elastic scattering cross section through $v(\mathbf{x}, t) = \int_{\mathbf{q}} \sigma(\mathbf{q}, t)(1 - e^{i\mathbf{q} \cdot \mathbf{x}})$.

Performing a full resummation of multiple interactions can be done employing numerical [66–71] or analytical techniques. For sufficiently dilute or small media, the probability of one scattering dominates [72–74]. On the contrary, for large or dense media, multiple scattering on the background medium start to play a role [61, 62, 75, 76]. In this case, there will be an interplay between copious, soft interactions and rare, hard momentum exchanges. The soft regime is governed by LPM interference effects [77–79], allowing for the possibility of rapid energy-degradation of the emitting particle. It is therefore of utmost importance to establish whether this regime is relevant for expanding media, where the density rapidly decays with proper time. In order to address this question, we will employ three resummation schemes that, in total, cover the whole emission phase space [55], see supplemental material for derivations.

The key quantity of the problem is the so-called jet quenching parameter $\hat{q}_0 = 4\pi\alpha_s^2 N_c n(t)$ which is a direct measure of the scattering density. In a widely used Gyulassy-Wang (GW) model for medium interactions, $\sigma(\mathbf{q}, t) = 4\pi\hat{q}_0(t)/(\mathbf{q}^2 + \mu^2)^2$ where μ is the screening mass [80], with $\Sigma(\mathbf{p}^2, t) = \hat{q}_0(t)/(\mathbf{p}^2 + \mu^2)$. The mean-free-path of this medium is then given by $\lambda(t) = 1/\Sigma(0, t) = \mu/\hat{q}_0(t)$. The temperature dependence mainly affects the density of scattering centers, $n \propto T^3$ [81]. In this section we derive completely generic expressions for the rate of medium-induced emissions, valid for *any* medium evolution model. The evolution of the relevant scales of the radiative process is summarized in Fig. 1b).

Early in the jet propagation, when the time is shorter than the local mean-free-path $t \ll \lambda(t)$, the probability of interacting with the medium is still small and we can truncate the conventional *opacity expansion* (OE) at first order to obtain,

$$\Gamma_{\text{OE}}(\omega, t) = \frac{2\bar{\alpha}}{\omega} \frac{1}{\lambda(t)} \mathcal{F}\left(\frac{\mu^2 t}{2\omega}\right), \quad (2)$$

with $\mathcal{F}(x) = \ln(x) + \gamma_E - \cos(x)\text{Ci}(x) + \sin(x)\left(\frac{\pi}{2} - \text{Si}(x)\right)$, with $\text{Ci}(x)$ and $\text{Si}(x)$ the cosine and sine integral functions. The characteristic scale is $\bar{\omega}_c(t) = \mu^2 t/2$.

At later times, $t \gg \lambda(t)$, multiple interactions have to be taken into account and the OE diverges for soft gluon emissions [55]. Since other resummation schemes are called for, we first derive the rate at first order in the *resummed opacity expansion* (ROE), which reads

$$\Gamma_{\text{ROE}}(\omega, t) = \bar{\alpha} \frac{\hat{q}_0(t)t}{\omega^2} \int_0^1 ds \Delta(t, st) f(u(1-s)). \quad (3)$$

where $u = \mu^2 t/(2\omega)$, $f(x) = \sin(x)\text{Ci}(x) + \cos(x)\left(\frac{\pi}{2} - \text{Si}(x)\right)$, and the elastic Sudakov factor reads $\Delta(t, t_0) = \exp\left[-\int_{t_0}^t dt' \Sigma(0, t')\right]$. The characteristic scale for the low-energy behavior is now the Bethe-Heitler frequency $\omega_{\text{BH}}(t) = \mu^2 \lambda(t)/2$.

For emissions with $\omega > \omega_{\text{BH}}(t)$ in the multiple-scattering regime, the so-called *improved* opacity expansion (IOE) is the most appropriate [55–60]. In this framework, we write the potential as $v(\mathbf{x}, t) \approx v_{\text{HO}}(\mathbf{x}, t) + \delta v(\mathbf{x}, t)$, where $v_{\text{HO}}(\mathbf{x}, t) = \hat{q}(t)\mathbf{x}^2/4$ and $\delta v(\mathbf{x}, t) = \hat{q}_0(t) \ln(1/(\mathbf{x}^2 Q^2))\mathbf{x}^2/4$, where Q^2 is a separation scale and $\mu_*^2 = \mu^2 e^{-1+2\gamma_E}/4$ for the GW model. Here, we also introduced a “dressed” jet parameter $\hat{q} = \hat{q}_0 \ln Q^2/\mu_*^2$.

Up to the second order in the IOE expansion, we find $\Gamma_{\text{IOE}}(\omega, t) = \Gamma_{\text{IOE}}^{(0)}(\omega, t) + \Gamma_{\text{IOE}}^{(1)}(\omega, t)$, with

$$\Gamma_{\text{IOE}}^{(0)}(\omega, t) = \frac{\bar{\alpha}\hat{q}(t)}{\omega^2}(-\text{Im})\text{Tan}(t), \quad (4)$$

$$\Gamma_{\text{IOE}}^{(1)}(\omega, t) = \frac{\bar{\alpha}\hat{q}_0(t)}{\omega^2}(-\text{Im})\text{Tan}(t) \ln \frac{\omega \text{Cot}(t)}{2ie^{-\gamma_E} Q^2}, \quad (5)$$

where the characteristic scale is $\omega_c(t) = \hat{q}(t)t^2/2$. Here, $\text{Tan}(t) = S(t, 0)/C(0, t)$ where $S(t, t_0)$ and $C(t, t_0)$ are two characteristic solutions of the harmonic equation $[\partial_t^2 + \Omega(t)]f(t, t_0) = 0$, where $\Omega(t) = \sqrt{-i\hat{q}(t)/(2\omega)}$, with appropriate boundary conditions [82].

In order to proceed, we need to find a suitable matching scale Q^2 . For expanding media, the soft rate becomes explicitly time-dependent, and we have to fix the scale at the level of the rate rather than the level of the spectrum, as done before [58]. In the limit of soft gluon emissions, the IOE rate converges to a series in \hat{q}_0/\hat{q} where the leading order term is the well-known BDMPS-Z result. In this regime, the rate is quasi-instantaneous and we find that the higher-order (next-to-harmonic) corrections scale as

$$\frac{\Gamma_{\text{IOE}}^{(1)}}{\Gamma_{\text{IOE}}^{(0)}} \Big|_{\omega \gg \omega_c(t)} = \frac{\hat{q}_0}{\hat{q}} \left[\gamma_E + \frac{\pi}{4} - \frac{3}{2} \ln 2 + \ln \frac{\sqrt{\hat{q}(t)\omega}}{Q^2} \right]. \quad (6)$$

We obtain a time-dependent matching scale, that simply reads $Q^2(t) = \sqrt{\hat{q}(t)\omega}$. The rate at next-to-harmonic order therefore becomes in the soft limit

$$\Gamma_{\text{IOE}}(\omega, t)|_{\omega \ll \omega_c(t)} = \bar{\alpha} \sqrt{\frac{\hat{q}_{\text{eff}}(t)}{\omega^3}}, \quad (7)$$

where the effective jet transport parameter becomes $\hat{q}_{\text{eff}}(t) = \hat{q}(t)(1 + 0.646/\ln \frac{Q^2(t)}{\mu_*^2} + \dots)$ [83]. The implicit equation for the matching scale can only be satisfied above some minimal energy which is compatible with the Bethe-Heitler scale, i.e. $\omega > 2\mu_*^4 e/\hat{q}_0(t) \sim \omega_{\text{BH}}(t)$. This implies that the IOE should be matched onto the soft limit of the ROE at ultra-soft energies.

In the hard limit, the first order is strongly suppressed and the leading behavior is contained in the second term which leads to

$$\Gamma_{\text{IOE}}(\omega, t)|_{\omega \gg \omega_c(t)} = \bar{\alpha} \frac{\pi}{2} \frac{\hat{q}_0(t)t}{\omega^2}, \quad (8)$$

and is identical to the hard limit of the opacity expansion.

The rates derived above hold for any medium expansion model. However, in order to interpolate between both of the two cases of medium thermalization described

in the introduction, we assume that the temperature behaves parametrically as $T(t) = T_0[t_m/(t + t_m)]^{\alpha/3}$. The concrete models under consideration is therefore defined as

$$\hat{q}_0(t) = \begin{cases} \hat{q}_0 \left(\frac{t_m}{t+t_m} \right)^\alpha & \text{for model (i)}, \\ \hat{q}_0 \Theta(t - t_m) \left(\frac{t_m}{t} \right)^\alpha & \text{for model (ii)}. \end{cases} \quad (9)$$

where \hat{q}_0 defines a constant reference density in the two models, at $t = 0$ and $t = t_m$ respectively. A medium diluting according to a 1D Bjorken expansion corresponds to $\alpha = 1$, see above, but other cases can also be implemented in realistic phenomenological situations [70]. In this case, in order for $\omega_c(t) \gg \omega_{\text{BH}}(t)$, we then have to demand that

$$1 \ll \frac{t}{\lambda_0} \left(\frac{t_m}{t} \right)^\alpha, \quad (10)$$

where $\lambda_0 = \mu^2/\hat{q}_0$ is the mean-free-path at $t = 0$. For instance, in the Bjorken scenario, where $\alpha = 1$, the medium “hydrodynamization” time should be much bigger than the mean-free-path $t_m \gg \lambda$ in order to get contributions from this regime [84]. For our numerical studies in Fig. 2, we have chosen $\hat{q}_0 = 0.3 \text{ GeV}^3$, $\mu^2 = 0.09 \text{ GeV}^2$, similar to previous studies [85], and $t_m = 1 \text{ fm}$. We note that for $t < \lambda_0$, corresponding to early emissions in a dilute medium, the medium expansion has no significant effect and the single scattering (OE) rates are valid in that regime. For $t > \lambda_0$, the impact of expansion on both quenching models is substantial across all resummation schemes, which are matched through time-dependent kinematic scales.

The results for model (ii) are easily derived from the explicit results derived for model (i), merely by taking care of the matching condition to the vacuum at $t < t_m$. For example, at leading HO order in the IOE, $C(0, L) \mapsto \tilde{C}(t_m, L) + t_m \partial_L \tilde{C}(L, t_m)$. Crucially, Eq. (7) also holds for model (ii).

So far we have kept the screening mass constant, but here we briefly comment on the case of a time-dependent screening mass, i.e. $\mu(t) = \mu_0[t_m/(t + t_m)]^{\alpha/3}$. This effect is straightforwardly implemented in OE and ROE, while for IOE it brings a logarithmic correction to $\hat{q}(t)$. A decaying screening mass will most significantly affect soft gluon emissions. The energy scale in the dilute regime is slowly decaying, $\bar{\omega}_c(t) \propto [t_m/(t + t_m)]^{2\alpha/3} t$, but this is a small effect as long as t_m is large compared to the initial mean-free-path $\lambda_0 = \mu_0^2/\hat{q}_0$. More strikingly, the Bethe-Heitler energy will now decrease with time, $\omega_{\text{BH}}(t) \propto [t_m/(t + t_m)]^{\alpha/3}$. The matching scale $\bar{\omega}_c(t)$ now also decreases with time, and in some cases, the medium may dilute rapidly enough to never enter the multiple-scattering regime. Apart from this case, for larger gluon energies we expect the corrections to be small, e.g. note that the $\omega \gg \omega_c(t)$ behavior in (8) is insensitive to the screening mass.

Phenomenological applications. The medium-induced spectrum gives rise to energy loss which affects the overall suppression of high- p_T particles or jets, quantified

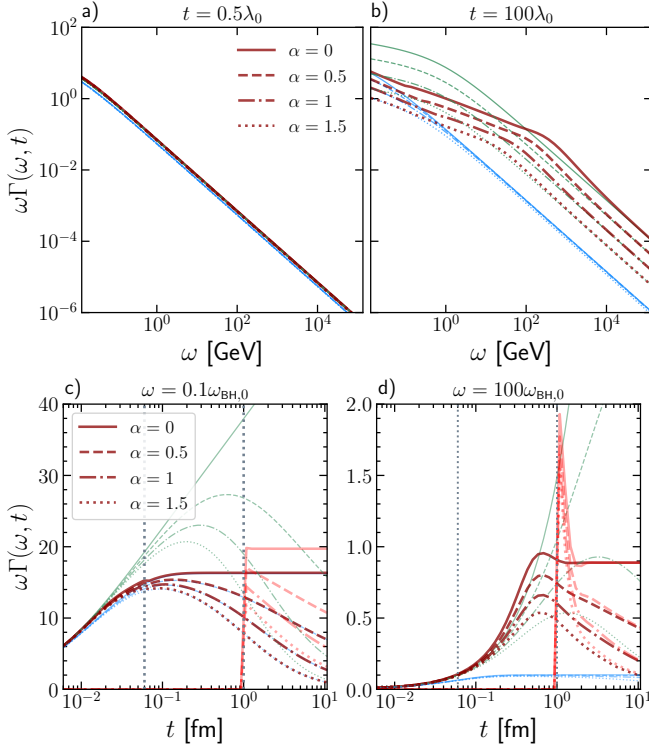


FIG. 2: The energy, in a) and b), and time, in c) and d), dependence of $\Gamma(\omega, t)$. Red curves correspond to the full result for model (i), while green (blue) curves represent the first-order OE and ROE results for reference, see also Fig. 1. Light-red curves are obtained for model (ii). Dotted black lines correspond to λ_0 and t_m values.

through the nuclear suppression factor R_{AA} , and to the azimuthal asymmetry of this suppression, quantified through the v_2 coefficient. To address the question that motivated our work, we propose an experimental observable that is sensitive to the medium's evolution during its earliest stages. To simplify the analysis we consider fully coherent jets, i.e. jets whose opening angle is smaller than the critical resolution angle in the medium [86]. In this case, the medium interactions can only resolve the total color charge of the jet and energy loss proceeds as off a single parton. This occurs for semi-central collisions at RHIC and LHC where the critical angle can be sizable [85, 87].

The quenching factor for a single parton due to radiative energy loss, which basically is the ratio of jet spectra in the presence and absence of medium effects, $\mathcal{Q}(p_T) = R_{AA}$, is well approximated by $-\ln \mathcal{Q} \simeq \int_0^L dt \int_{p_T/n}^\infty d\omega \Gamma(\omega, t)$ where n is the slope of the hard spectrum and $L = 5$ fm is the medium length [88]. For high-energy hadronic collisions, where typically $n \gtrsim 5.5$,

this immediately indicates that the Bethe-Heitler regime is not relevant for jet quenching at $p_T \gtrsim 10$ GeV. The azimuthal asymmetry of this quenching, for semi-central collisions, is readily found to be [85] $v_2/e \simeq -\frac{1}{2} d \ln \mathcal{Q} / d \ln L = \frac{1}{2} L \int_{p_T/n}^\infty d\omega \Gamma(\omega, L)$, where e is the ellipticity of the nuclear overlap. While the quenching factor is sensitive to the accumulation of emissions along the entire in-medium path length L , the v_2 coefficient is directly sensitive to the rate at late times.

Emissions belonging to the multiple-scattering regime, see Eq. (7), lead to a sizable suppression factors $\mathcal{Q} \ll 1$ due to the high multiplicity of emissions [88], see also [55]. Considering the two models of expanding media defined in Eq. (9), we readily obtain

$$\frac{v_2^{\text{soft}}}{e} = \ln \frac{1}{\mathcal{Q}^{\text{soft}}} \begin{cases} \left(\frac{x_m/(1+x_m)}{\Phi_1(x_m; \alpha/2)} \right)^{\alpha/2} & \text{for (i)} \\ \frac{x_m^{\alpha/2}}{\Phi_2(x_m; \alpha/2)} & \text{for (ii)} \end{cases}, \quad (11)$$

where $x_m \equiv t_m/L$ and we have neglected slow, logarithmic contributions and evaluate \hat{q} at L . For scenario (i), we get $\Phi_1(x; \alpha) = \frac{x^\alpha}{1-\alpha} ((1+x)^{1-\alpha} - x^{1-\alpha})$ and $x = t_m/L$, while for scenario (ii) we arrive at $\Phi_2(x; \alpha) = \frac{x^\alpha}{1-\alpha} (1 - x^{1-\alpha})$. The enhancement factor on the right-hand side, obtained within these approximations, is p_T -independent and, as a consequence, fixing the quenching factor \mathcal{Q} , we deduce that $v_2^{(i)} < v_2^{(ii)}$ for any $0 < x_m < 1$ and for any $\alpha \geq 0$.

We have evaluated numerically the quenching factors $\mathcal{Q}(p_T)$ and azimuthal coefficients v_2/e in Fig. 3 for the full, interpolated rate valid in all regimes for the same set of parameters as used above (the plotted observables are the nuclear suppression factor \mathcal{Q} (leftmost panel), the azimuthal coefficient v_2/e (center panel) and their ratio (rightmost panel)). For different medium-evolution scenarios a weak p_T -dependence appears due to the evolving separation scale $\omega_c(t)$, and we observe that this can affect the relative weight of accumulated and late quenching as contained in $\ln 1/\mathcal{Q}$ and v_2/e , respectively. The distinction in terms of geometry and resulting evolving scales in momentum scales between these two observables, could become an important tool to pin down the early evolution of \hat{q} in heavy-ion collisions.

Acknowledgements: SPA acknowledges funding from grant agreement PAN.BFD.S.BDN.612.022.2021-PASIFIC 1, QGPAnatomy and Physics for Future (P4F) Project No. 101081515, PEAKIN. This work received funding from the European Union's Horizon 2020 research and innovation program under the Maria Skłodowska-Curie grant agreement No. 847639, the Polish Ministry of Education, the Horizon Europe Programme, HORIZON-MSCA-2021-COFUND-01 call by the European Research Executive Agency.

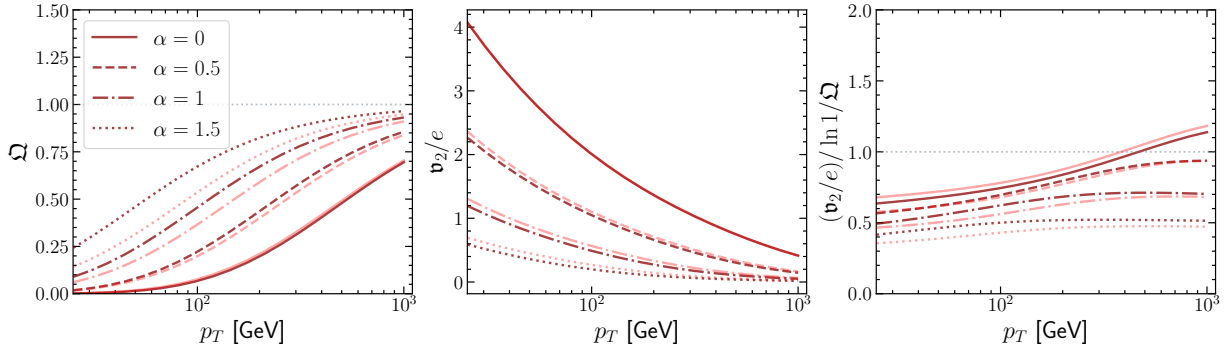


FIG. 3: Enhancement of jet v_2 at fixed parton suppression factor between model (ii) and (i). Curves from bottom to top correspond to different expansion with $0 \leq \alpha < 1.75$. An enhancement of 20% is achieved for $x_m \approx 0.15$.

-
- [1] R. K. Ellis, W. J. Stirling, and B. R. Webber, *QCD and collider physics*, Vol. 8 (Cambridge University Press, 2011).
- [2] Y. L. Dokshitzer, V. A. Khoze, A. H. Mueller, and S. I. Troian, *Basics of perturbative QCD* (1991).
- [3] M. Gyulassy and M. Plumer, *Phys. Lett. B* **243**, 432 (1990).
- [4] M. Gyulassy, I. Vitev, X.-N. Wang, and B.-W. Zhang, *Phys. Lett. B* **592**, 123 (2004), arXiv:nucl-th/0302077.
- [5] S. Peigne and A. V. Smilga, *Phys. Usp.* **52**, 659 (2009), arXiv:0810.5702 [hep-ph].
- [6] Y. Mehtar-Tani, J. G. Milhano, and K. Tywoniuk, *Int. J. Mod. Phys. A* **28**, 1340013 (2013), arXiv:1302.2579 [hep-ph].
- [7] J. Ghiglieri and D. Teaney, *Int. J. Mod. Phys. E* **24**, 1530013 (2015), arXiv:1502.03730 [hep-ph].
- [8] H. A. Andrews *et al.*, *J. Phys. G* **47**, 065102 (2020), arXiv:1808.03689 [hep-ph].
- [9] C. Adler *et al.* (STAR), *Phys. Rev. Lett.* **90**, 082302 (2003), arXiv:nucl-ex/0210033.
- [10] J. Adams *et al.* (STAR), *Phys. Rev. Lett.* **91**, 072304 (2003), arXiv:nucl-ex/0306024.
- [11] G. Aad *et al.* (ATLAS), *Phys. Rev. Lett.* **105**, 252303 (2010), arXiv:1011.6182 [hep-ex].
- [12] S. Chatrchyan *et al.* (CMS), *Phys. Rev. C* **84**, 024906 (2011), arXiv:1102.1957 [nucl-ex].
- [13] G. Aad *et al.* (ATLAS), *Phys. Lett. B* **719**, 220 (2013), arXiv:1208.1967 [hep-ex].
- [14] B. Abelev *et al.* (ALICE), *JHEP* **03**, 013, arXiv:1311.0633 [nucl-ex].
- [15] G. Aad *et al.* (ATLAS), *Phys. Rev. Lett.* **114**, 072302 (2015), arXiv:1411.2357 [hep-ex].
- [16] S. Chatrchyan *et al.* (CMS), *Phys. Rev. C* **90**, 024908 (2014), arXiv:1406.0932 [nucl-ex].
- [17] G. Aad *et al.* (ATLAS), *Phys. Lett. B* **739**, 320 (2014), arXiv:1406.2979 [hep-ex].
- [18] G. Aad *et al.* (ATLAS), *Phys. Lett. B* **751**, 376 (2015), arXiv:1506.08656 [hep-ex].
- [19] V. Khachatryan *et al.* (CMS), *JHEP* **11**, 055, arXiv:1609.02466 [nucl-ex].
- [20] V. Khachatryan *et al.* (CMS), *Phys. Rev. C* **96**, 015202 (2017), arXiv:1609.05383 [nucl-ex].
- [21] M. Aaboud *et al.* (ATLAS), *Eur. Phys. J. C* **77**, 379 (2017), arXiv:1702.00674 [hep-ex].
- [22] M. Aaboud *et al.* (ATLAS), *Phys. Lett. B* **774**, 379 (2017), arXiv:1706.09363 [hep-ex].
- [23] M. Aaboud *et al.* (ATLAS), *Phys. Lett. B* **790**, 108 (2019), arXiv:1805.05635 [nucl-ex].
- [24] S. Acharya *et al.* (ALICE), *Phys. Rev. C* **101**, 034911 (2020), arXiv:1909.09718 [nucl-ex].
- [25] G. Aad *et al.* (ATLAS), *Phys. Rev. C* **105**, 064903 (2022), arXiv:2111.06606 [nucl-ex].
- [26] M. S. Abdallah *et al.* (STAR), *Phys. Rev. C* **105**, 044906 (2022), arXiv:2109.09793 [nucl-ex].
- [27] G. Aad *et al.* (ATLAS), *Phys. Rev. C* **107**, 054909 (2023), arXiv:2211.11470 [nucl-ex].
- [28] G. Aad *et al.* (ATLAS), *Phys. Rev. C* **107**, 054908 (2023), [Erratum: *Phys. Rev. C* **109**, 029901 (2024)], arXiv:2205.00682 [nucl-ex].
- [29] S. Acharya *et al.* (ALICE), *JHEP* **05**, 245, arXiv:2204.10270 [nucl-ex].
- [30] S. Acharya *et al.* (ALICE), *Phys. Rev. C* **110**, 014906 (2024), arXiv:2308.16128 [nucl-ex].
- [31] G. Aad *et al.* (ATLAS), *Phys. Rev. Lett.* **131**, 172301 (2023), arXiv:2301.05606 [nucl-ex].
- [32] N. Armesto and E. Scapparini, *Eur. Phys. J. Plus* **131**, 52 (2016), arXiv:1511.02151 [nucl-ex].
- [33] M. Connors, C. Nattrass, R. Reed, and S. Salur, *Rev. Mod. Phys.* **90**, 025005 (2018), arXiv:1705.01974 [nucl-ex].
- [34] R. Kogler *et al.*, *Rev. Mod. Phys.* **91**, 045003 (2019), arXiv:1803.06991 [hep-ex].
- [35] L. Cunqueiro and A. M. Sickles, *Prog. Part. Nucl. Phys.* **124**, 103940 (2022), arXiv:2110.14490 [nucl-ex].
- [36] L. Apolinário, Y.-J. Lee, and M. Winn, *Prog. Part. Nucl. Phys.* **127**, 103990 (2022), arXiv:2203.16352 [hep-ph].
- [37] H. Song, S. A. Bass, U. Heinz, T. Hirano, and C. Shen, *Phys. Rev. Lett.* **106**, 192301 (2011), [Erratum: *Phys. Rev. Lett.* **109**, 139904 (2012)], arXiv:1011.2783 [nucl-th].
- [38] J. D. Bjorken, *Phys. Rev. D* **27**, 140 (1983).
- [39] S. P. Adhya, C. A. Salgado, M. Spousta, and K. Tywoniuk, *JHEP* **07**, 150, arXiv:1911.12193 [hep-ph].
- [40] P. Caucal, E. Iancu, A. H. Mueller, and G. Soyez, *JHEP* **10**, 204, arXiv:2005.05852 [hep-ph].

- [41] S. P. Adhya, C. A. Salgado, M. Spousta, and K. Tywoniuk, *Eur. Phys. J. C* **82**, 20 (2022), [arXiv:2106.02592 \[hep-ph\]](#).
- [42] S. P. Adhya, K. Kutak, W. Placzek, M. Rohrmoser, and K. Tywoniuk, *Eur. Phys. J. C* **83**, 512 (2023), [arXiv:2211.15803 \[hep-ph\]](#).
- [43] A. H. Mueller, *Phys. Lett. B* **475**, 220 (2000), [arXiv:hep-ph/9909388](#).
- [44] R. Baier, A. H. Mueller, D. Schiff, and D. T. Son, *Phys. Lett. B* **502**, 51 (2001), [arXiv:hep-ph/0009237](#).
- [45] J. Berges, K. Boguslavski, S. Schlichting, and R. Venugopalan, *Phys. Rev. D* **89**, 074011 (2014), [arXiv:1303.5650 \[hep-ph\]](#).
- [46] J. Berges, K. Boguslavski, S. Schlichting, and R. Venugopalan, *Phys. Rev. D* **89**, 114007 (2014), [arXiv:1311.3005 \[hep-ph\]](#).
- [47] A. Kurkela and Y. Zhu, *Phys. Rev. Lett.* **115**, 182301 (2015), [arXiv:1506.06647 \[hep-ph\]](#).
- [48] A. Ipp, D. I. Müller, and D. Schuh, *Phys. Rev. D* **102**, 074001 (2020), [arXiv:2001.10001 \[hep-ph\]](#).
- [49] A. Ipp, D. I. Müller, and D. Schuh, *Phys. Lett. B* **810**, 135810 (2020), [arXiv:2009.14206 \[hep-ph\]](#).
- [50] M. E. Carrington, A. Czajka, and S. Mrowczynski, *Phys. Lett. B* **834**, 137464 (2022), [arXiv:2112.06812 \[hep-ph\]](#).
- [51] M. E. Carrington, A. Czajka, and S. Mrowczynski, *Phys. Rev. C* **105**, 064910 (2022), [arXiv:2202.00357 \[nucl-th\]](#).
- [52] D. Avramescu, V. Baran, V. Greco, A. Ipp, D. I. Müller, and M. Ruggieri, *Phys. Rev. D* **107**, 114021 (2023), [arXiv:2303.05599 \[hep-ph\]](#).
- [53] J. Barata, S. Hauksson, X. Mayo López, and A. V. Sadofyev, (2024), [arXiv:2406.07615 \[hep-ph\]](#).
- [54] In most works on hard probes in glasma, one actually studies the momentum broadening of particles. For a discussion of the modified radiative spectrum, see e.g. [53].
- [55] J. H. Isaksen, A. Takacs, and K. Tywoniuk, *JHEP* **02**, 156, [arXiv:2206.02811 \[hep-ph\]](#).
- [56] Y. Mehtar-Tani, *JHEP* **07**, 057, [arXiv:1903.00506 \[hep-ph\]](#).
- [57] Y. Mehtar-Tani and K. Tywoniuk, *JHEP* **06**, 187, [arXiv:1910.02032 \[hep-ph\]](#).
- [58] J. Barata and Y. Mehtar-Tani, *JHEP* **10**, 176, [arXiv:2004.02323 \[hep-ph\]](#).
- [59] J. Barata, Y. Mehtar-Tani, A. Soto-Ontoso, and K. Tywoniuk, *Phys. Rev. D* **104**, 054047 (2021), [arXiv:2009.13667 \[hep-ph\]](#).
- [60] J. Barata, Y. Mehtar-Tani, A. Soto-Ontoso, and K. Tywoniuk, *JHEP* **09**, 153, [arXiv:2106.07402 \[hep-ph\]](#).
- [61] R. Baier, Y. L. Dokshitzer, A. H. Mueller, S. Peigne, and D. Schiff, *Nucl. Phys. B* **483**, 291 (1997), [arXiv:hep-ph/9607355](#).
- [62] B. G. Zakharov, *JETP Lett.* **65**, 615 (1997), [arXiv:hep-ph/9704255](#).
- [63] P. B. Arnold, G. D. Moore, and L. G. Yaffe, *JHEP* **06**, 030, [arXiv:hep-ph/0204343](#).
- [64] F. Dominguez, C. Marquet, A. M. Stasto, and B.-W. Xiao, *Phys. Rev. D* **87**, 034007 (2013), [arXiv:1210.1141 \[hep-ph\]](#).
- [65] We have also introduced the notation for transverse integrals, where $\int_q = \int d^2q/(2\pi)^2$ and $\int_x = \int d^2x$.
- [66] B. G. Zakharov, *JETP Lett.* **80**, 617 (2004), [arXiv:hep-ph/0410321](#).
- [67] S. Caron-Huot and C. Gale, *Phys. Rev. C* **82**, 064902 (2010), [arXiv:1006.2379 \[hep-ph\]](#).
- [68] X. Feal and R. Vazquez, *Phys. Rev. D* **98**, 074029 (2018), [arXiv:1811.01591 \[hep-ph\]](#).
- [69] W. Ke, Y. Xu, and S. A. Bass, *Phys. Rev. C* **100**, 064911 (2019), [arXiv:1810.08177 \[nucl-th\]](#).
- [70] C. Andres, L. Apolinário, and F. Dominguez, *JHEP* **07**, 114, [arXiv:2002.01517 \[hep-ph\]](#).
- [71] S. Schlichting and I. Soudi, *JHEP* **07**, 077, [arXiv:2008.04928 \[hep-ph\]](#).
- [72] M. Gyulassy, P. Levai, and I. Vitev, *Nucl. Phys. B* **571**, 197 (2000), [arXiv:hep-ph/9907461](#).
- [73] U. A. Wiedemann, *Nucl. Phys. B* **588**, 303 (2000), [arXiv:hep-ph/0005129](#).
- [74] M. D. Sievert and I. Vitev, *Phys. Rev. D* **98**, 094010 (2018), [arXiv:1807.03799 \[hep-ph\]](#).
- [75] C. A. Salgado and U. A. Wiedemann, *Phys. Rev. D* **68**, 014008 (2003), [arXiv:hep-ph/0302184](#).
- [76] N. Armesto, C. A. Salgado, and U. A. Wiedemann, *Phys. Rev. D* **69**, 114003 (2004), [arXiv:hep-ph/0312106](#).
- [77] L. L. D. and P. I., *Dokl. Akad. Nauk Ser. Fiz.* **92**, 535 (1953).
- [78] L. L. D. and P. I., *Dokl. Akad. Nauk Ser. Fiz.* **92**, 735 (1953).
- [79] A. B. Migdal, *Phys. Rev.* **103**, 1811 (1956).
- [80] X.-N. Wang and M. Gyulassy, *Phys. Rev. Lett.* **68**, 1480 (1992).
- [81] In a thermal medium, the in-medium screening mass is temperature dependent, $\mu^2 \propto T^2$, but we will neglect this effect since it only gives rise to logarithmic corrections for emissions at the thermal scale, $\omega \sim T$, and comment on the expected effects below.
- [82] P. B. Arnold, *Phys. Rev. D* **79**, 065025 (2009), [arXiv:0808.2767 \[hep-ph\]](#).
- [83] It is worth pointing out that our results are slightly different from previous calculations of the IOE rate and spectrum, in particular [58]. The reason for the discrepancy is the incomplete subtraction of vacuum contributions, leading to an additional term $\propto \partial_s C(s, L)/C(s, L)$ in previous works, which does not appear when we fully subtract the vacuum contribution, as done in Eq. (1).
- [84] The limit $t_m < \lambda_0$ is not of phenomenological relevance as for the hydrodynamic modes to set in the regime, one needs a reasonable mean-free-path to avoid instantaneous interactions. For our parameters $t_m \gg \lambda_0$. In any case, OE captures the dynamics in this regime.
- [85] Y. Mehtar-Tani, D. Pablos, and K. Tywoniuk, (2024), [arXiv:2402.07869 \[hep-ph\]](#).
- [86] J. Casalderrey-Solana, Y. Mehtar-Tani, C. A. Salgado, and K. Tywoniuk, *Phys. Lett. B* **725**, 357 (2013), [arXiv:1210.7765 \[hep-ph\]](#).
- [87] Y. Mehtar-Tani, D. Pablos, and K. Tywoniuk, *Phys. Rev. Lett.* **127**, 252301 (2021), [arXiv:2101.01742 \[hep-ph\]](#).
- [88] R. Baier, Y. L. Dokshitzer, A. H. Mueller, and D. Schiff, *JHEP* **09**, 033, [arXiv:hep-ph/0106347](#).
- [89] E. Iancu, *JHEP* **10**, 095, [arXiv:1403.1996 \[hep-ph\]](#).
- [90] H. Kleinert, (2004).

SUPPLEMENTAL MATERIAL

1. 3-point function in expanding medium

In order to address this question, we will employ the so-called *improved* opacity expansion (IOE) [55–60]. In this framework, we write the potential as $v(\mathbf{x}, t) \approx v_{\text{HO}}(\mathbf{x}, t) + \delta v(\mathbf{x}, t) + \dots$, where $v_{\text{HO}}(\mathbf{x}, t) = \mathbf{x}^2 \hat{q}(t)/4$ and $\delta v(\mathbf{x}, t) = (\hat{q}_0(t)/4) \mathbf{x}^2 \ln(1/(\mathbf{x}^2 Q^2))$, where Q^2 is a separation scale. This scale ensures that the first term dominates, i.e. we assume $Q^2 \gg \mu_*^2$, and is set by demanding a universal behavior in the soft limit of the spectrum [58, 89]. This allows to define a “dressed” medium transport parameter $\hat{q}(t) \equiv \hat{q}_0(t) \ln Q^2/\mu_*^2$.

The expansion of the full 3-point correlator $\mathcal{K}(\mathbf{x}, \mathbf{y})$ can be cast as an implicit equation,

$$\mathcal{K}(\mathbf{x}, t_2; \mathbf{y}, t_1) = \mathcal{K}_{\text{HO}}(\mathbf{x}, t_2; \mathbf{y}, t_1) - \int_{\mathbf{z}} \int_{t_1}^{t_2} ds \mathcal{K}_{\text{HO}}(\mathbf{x}, t_2; \mathbf{z}, s) \delta v(\mathbf{z}, s) \mathcal{K}(\mathbf{z}, s; \mathbf{y}, t_1), \quad (12)$$

where $\mathcal{K}_{\text{HO}}(\mathbf{x}, \mathbf{y})$ is the full correlator with the harmonic potential $v_{\text{HO}}(\mathbf{x}, t)$. The exact solution then reads [82, 90],

$$\mathcal{K}_{\text{HO}}(\mathbf{x}, t_2; \mathbf{y}, t_1) = \frac{\omega}{2\pi i S(t_2, t_1)} \exp \left\{ \frac{i\omega}{2S(t_2, t_1)} \times \left[C(t_1, t_2) \mathbf{x}^2 + C(t_2, t_1) \mathbf{y}^2 - 2\mathbf{x} \cdot \mathbf{y} \right] \right\}. \quad (13)$$

The functions $C(t, t_0)$ and $S(t, t_0)$ both satisfy the harmonic equation $[\partial_t^2 + \Omega^2(t)]f(t, t_0) = 0$, where $\Omega^2(t) = -i\hat{q}(t)/(2\omega)$. The two sets of different boundary conditions are $S(t_0, t_0) = 0$ and $\partial_t S(t, t_0)|_{t=t_0} = 1$ and $C(t_0, t_0) = 1$ and $\partial_t C(t, t_0)|_{t=t_0} = 0$, respectively. These solutions are related by the associated Wronskian, which reads $W = C(t, t_0)\partial_t S(t, t_0) - S(t, t_0)\partial_t C(t, t_0) = 1$ for the above initial conditions. This implies that $S(t, t_0) = -S(t_0, t)$.

a. Vacuum solutions: The vacuum solutions for the two functions are enforced by the boundary conditions and are simply $S(t, t_0) = t - t_0$ and $C(t, t_0) = 1$.

b. Medium with constant density: With a constant density, $\hat{q}(t) = \hat{q}$, the solutions are well known $S(t, t_0) = \sin[\Omega(t - t_0)]/\Omega$ and $C(t, t_0) = \cos[\Omega(t - t_0)]$, where $\Omega = \sqrt{-i\hat{q}/(2\omega)}$.

c. Expanding medium (scenario 1): The first scenario suggested in the paper, proposes a medium that continuously is decaying from a constant value, namely $\hat{q}(t) = \hat{q}[t_m/(t + t_m)]^\alpha$. Defining $\nu = 1/(2 - \alpha)$ and introducing the combined variable $z_t = 2i\nu\Omega t_m[(t +$

$t_m)/t_m]^{1/2\nu}$, we can write them as

$$S(t, t_0) = 2\nu \sqrt{(t + t_m)(t_0 + t_m)} \times \left[I_\nu(z_t) K_\nu(z_{t_0}) - I_\nu(z_{t_0}) K_\nu(z_t) \right], \quad (14)$$

$$C(t, t_0) = 2i\nu\Omega \sqrt{t + t_m}(t_0 + t_m)^{\frac{1-\nu}{2\nu}} \times \left[I_\nu(z_t) K_{\nu-1}(z_{t_0}) + I_{\nu-1}(z_{t_0}) K_\nu(z_t) \right]. \quad (15)$$

d. Expanding medium (scenario 2): The second scenario suggested in the paper, consists of a vacuum-like phase up to a medium thermalization time t_m , i.e. $\hat{q}(t) = 0$ for $t < t_m$, and a decaying medium afterwards, i.e. $\hat{q}(t) = \hat{q}(t_m/t)^\alpha$ for $t \geq t_m$. Since for a time ordered $t > t_1 > t_0$, any solution in (t_2, t_1) can be written as [82], $S(t, t_0) = C(t_0, t_1)S(t, t_1) - S(t_0, t_1)C(t, t_1)$ and $C(t, t_0) = -\partial_{t_0} C(t_0, t_1)S(t, t_1) + \partial_{t_0} S(t_0, t_1)C(t, t_1)$. By assigning the intermediate time t_1 to t_m , and utilizing the vacuum solutions for the $(0, t_m)$ interval, we find

$$S(t, 0) = \tilde{S}(t, t_m) + t_m \tilde{C}(t, t_m), \quad (16)$$

$$C(0, t) = \tilde{C}(t_m, t) + t_m \partial_t \tilde{C}(t, t_m), \quad (17)$$

where $\tilde{S}(t, t_0)$ and $\tilde{C}(t, t_0)$ can be read off Eqs. (14) and (15) by substituting $t + t_m \rightarrow t$ and $t_0 + t_m \rightarrow t_0$. Hence, the corrections are of order t_m and does not affect the soft behavior of the functions.

e. Generic solutions: Assuming that the solutions to $S(t, t_0)$ and $C(t, t_0)$ are the linear combinations of two independent solutions to the second-order differential equations, i.e. $c_1 f_1(t) + c_2 f_2(t)$, we find

$$S(t, t_0) = \frac{1}{\Phi(t_0)} \left(\frac{f_1(t)}{f_1(t_0)} - \frac{f_2(t)}{f_2(t_0)} \right), \quad (18)$$

$$C(t, t_0) = \frac{1}{\Phi(t_0)} \left(-[\partial_t \ln f_2(t)]_{t=t_0} \frac{f_1(t)}{f_1(t_0)} + [\partial_t \ln f_1(t)]_{t=t_0} \frac{f_2(t)}{f_2(t_0)} \right), \quad (19)$$

where we defined $\Phi(t_0) = [\partial_t \ln f_1(t) - \partial_t \ln f_2(t)]_{t=t_0}$.

2. Calculating the medium-induced rate

The rate $\Gamma(\omega, t) = dI/(d\omega dt)$ can also be directly evaluated from the following form [55, 64]

$$\Gamma(\omega, t) = \frac{4\bar{\alpha}\pi}{\omega^2} \int_0^t dt_0 \int_{\mathbf{p}, \mathbf{p}_0} \Sigma(\mathbf{p}^2, t) \frac{\mathbf{p} \cdot \mathbf{p}_0}{\mathbf{p}^2} \times (-\text{Im}) \mathcal{K}(\mathbf{p}, t; \mathbf{p}_0, t_0), \quad (20)$$

where $\Sigma(\mathbf{p}^2, t) = \int_{\mathbf{q}} \Theta(\mathbf{q}^2 - \mathbf{p}^2) \sigma(\mathbf{q}, t)$. For the GW potential, we have

$$\Sigma(\mathbf{k}^2, t) = \frac{\hat{q}_0(t)}{\mathbf{k}^2 + \mu^2}, \quad (21)$$

where $\hat{q}_0(s) = 4\pi\alpha_s^2 N_c n(s)$ is a measure of the scattering density. We will also define the (time-dependent) mean free path as $\Sigma(0, t) \equiv \lambda^{-1}(t)$.

a. Opacity expansion: In the opacity expansion (OE), the 3-point functions is expanded around the vacuum solution, symbolically $\mathcal{K}(\mathbf{p}; \mathbf{p}_0) = (2\pi)^2 \delta(\mathbf{p} - \mathbf{p}_0) \mathcal{K}_0(\mathbf{p}) - \int_{\mathbf{q}} \mathcal{K}_0(\mathbf{p}) v(\mathbf{q}) \mathcal{K}(\mathbf{p} - \mathbf{q}; \mathbf{p}_0)$ where the interaction $v(\mathbf{q}) = (2\pi)^2 \delta(\mathbf{q}) \Sigma(0, s) - \sigma(\mathbf{q}, s)$ occurs at some intermediate time s , to be summed over, and we have suppressed the time-variables for simplicity. The vacuum propagator is simply $\mathcal{K}_0(\mathbf{p}) = \exp[-i\frac{\mathbf{p}^2}{2\omega}(t - t_0)]$.

The rate at first order in opacity can be written as

$$\Gamma_{\text{OE}}(\omega, t) = \frac{2\bar{\alpha}}{\lambda(t)\omega} \mathcal{F}\left(\frac{\bar{\omega}_c(t)}{\omega}\right), \quad (22)$$

where $\mathcal{F}(x) = \ln(x) + \gamma_E - \cos(x)\text{Ci}(x) + \sin(x)(\frac{\pi}{2} - \text{Si}(x))$, with $\text{Ci}(x)$ and $\text{Si}(x)$ the cosine and sine integral functions. The energy scale is found to be $\bar{\omega}_c(t) = \mu^2 t/2$. This immediately implies the limiting behavior for the rate, as

$$\Gamma_{\text{OE}}(\omega, t) = \frac{2\bar{\alpha}}{\lambda(t)\omega} \begin{cases} \ln \frac{\bar{\omega}_c(t)}{\omega} + \gamma_E & \text{for } \omega \ll \bar{\omega}_c(t), \\ \frac{\pi}{2} \frac{\bar{\omega}_c(t)}{\omega} & \text{for } \omega \gg \bar{\omega}_c(t), \end{cases} \quad (23)$$

b. Resummed opacity expansion: The resummed opacity expansion (ROE) expands the 3-point function as $\mathcal{K}(\mathbf{p}; \mathbf{p}_0) = (2\pi)^2 \delta(\mathbf{p} - \mathbf{p}_0) \Delta(t, t_0) \mathcal{K}_0(\mathbf{p}) - \int_{\mathbf{q}} \Delta(t, s) \mathcal{K}_0(\mathbf{p}) \sigma(\mathbf{q}) \mathcal{K}(\mathbf{p} - \mathbf{q}; \mathbf{p}_0)$, see [55]. Here, we have explicitly the elastic Sudakov form factor for a generic medium profile can be written as,

$$\Delta(t, t_0) \equiv e^{-\int_{t_0}^t ds \Sigma(0, s)}. \quad (24)$$

At first order in this expansion the ROE spectrum reads

$$\Gamma_{\text{ROE}}(\omega, t) = \bar{\alpha} \frac{\hat{q}_0(t)t}{\omega^2} \int_0^1 ds \Delta(t, st) f(u(1-s)), \quad (25)$$

where $u = \bar{\omega}_c(t)/\omega$ and $f(x) = \sin(x)\text{Ci}(x) + \cos(x)(\frac{\pi}{2} - \text{Si}(x))$. Given that the Sudakov factor is exponentially decaying, we can approximate $\Delta(t, t_0) \simeq e^{-(t-t_0)/\lambda(t)}$. The asymptotic limits can easily be obtained as,

$$\Gamma_{\text{ROE}}(\omega, t) \simeq \frac{2\bar{\alpha}}{\lambda(t)\omega} \begin{cases} \ln \frac{\omega_{\text{BH}}(t)}{\omega} + \text{Ei}\left(-\frac{t}{\lambda(t)}\right) & \text{for } \omega \rightarrow 0, \\ \frac{\pi}{2} \frac{\omega_{\text{BH}}(t)}{\omega} (1 - e^{-t/\lambda(t)}) & \text{for } \omega \rightarrow \infty, \end{cases} \quad (26)$$

where $\omega_{\text{BH}}(t) = \mu^2 \lambda(t)/2$. In the dilute case, $t \ll \lambda(t)$, we directly recover the OE results in Eq. (23) where the scale becomes $\bar{\omega}_c(t)$.

In the regime of multiple scattering, $t \gg \lambda(t)$, due to the transmutation of scales, we only relevant energy becomes $\omega_{\text{BH}}(t)$. We get

$$\Gamma_{\text{ROE}}(\omega, t) \simeq \frac{2\bar{\alpha}}{\lambda(t)\omega} \begin{cases} \ln \frac{\omega_{\text{BH}}(t)}{\omega} & \text{for } \omega \ll \omega_{\text{BH}}(t), \\ \frac{\pi}{2} \frac{\omega_{\text{BH}}(t)}{\omega} & \text{for } \omega \gg \omega_{\text{BH}}(t), \end{cases} \quad (27)$$

c. Improved opacity expansion: For the improved opacity expansion (IOE), we will use the expression for the rate, Eq. (20), Fourier transformed to transverse coordinate space [55, App. B],

$$\Gamma(\omega, t) = \frac{2\bar{\alpha}}{\omega^2} \int_0^t dt_0 \int_{\mathbf{z}} v(\mathbf{z}, t) \frac{\mathbf{z}}{z^2} \cdot \partial_{\mathbf{y}} \times (-\text{Im}) \mathcal{K}(\mathbf{z}, t; \mathbf{y}, t_0) \Big|_{\mathbf{y}=0}. \quad (28)$$

The medium potential is then separated as $v(\mathbf{z}, t) = v_{\text{HO}}(\mathbf{z}, t) + \delta v(\mathbf{z}, t)$, and the 3-point function is expanded as $\mathcal{K}(\mathbf{x}; \mathbf{y}) = \mathcal{K}_{\text{HO}}(\mathbf{x}; \mathbf{y}) - \int_{\mathbf{z}} \mathcal{K}_{\text{HO}}(\mathbf{x} - \mathbf{z}; \mathbf{y}) \delta v(\mathbf{z}) \mathcal{K}(\mathbf{z}; \mathbf{y})$. The first two terms in the expansion then reads,

$$\Gamma_{\text{IOE}}^{(0)}(\omega, t) = \frac{\bar{\alpha} \hat{q}(t)}{\omega^2} (-\text{Im}) \text{Tan}(t), \quad (29)$$

$$\Gamma_{\text{IOE}}^{(1)}(\omega, t) = \frac{\bar{\alpha} \hat{q}_0(t)}{\omega^2} (-\text{Im}) \text{Tan}(t) \ln \left[\frac{\omega \text{Cot}(t)}{2ie^{-\gamma_E} Q^2} \right], \quad (30)$$

where $\text{Tan}(t) = 1/\text{Cot}(t) \equiv \frac{S(t,0)}{C(0,t)}$. The soft limit of these rates follows straightforwardly from $\lim_{\omega \rightarrow 0} \text{Tan}(t) = (1-i)\sqrt{\omega/\hat{q}(t)}$, as

$$\lim_{\omega \rightarrow 0} \Gamma_{\text{IOE}}^{(0)}(\omega, t) = \bar{\alpha} \sqrt{\frac{\hat{q}(t)}{\omega^3}}, \quad (31)$$

$$\lim_{\omega \rightarrow 0} \Gamma_{\text{IOE}}^{(1)}(\omega, t) = \bar{\alpha} \frac{\hat{q}_0(t)}{\sqrt{\hat{q}(t)\omega^3}} \times \left[\ln \frac{\sqrt{\hat{q}(t)\omega}}{Q^2} + \gamma_E - \frac{3}{2} \ln 2 + \frac{\pi}{4} \right]. \quad (32)$$

In the hard limit, we obtain $\lim_{\omega \rightarrow \infty} \text{Tan}(t) = t + \mathcal{O}(1/\omega)$. The harmonic oscillator term therefore is strongly suppressed, $\Gamma_{\text{IOE}}^{(0)} \sim \mathcal{O}(1/\omega^3)$, and the leading behavior is contained in the second term which, using $\ln i = i\pi/2$, simply reads

$$\lim_{\omega \rightarrow \infty} \Gamma_{\text{IOE}}^{(1)}(\omega, t) = \bar{\alpha} \frac{\pi \hat{q}_0(t)t}{2\omega^2}, \quad (33)$$

and is identical to the hard limit of the opacity expansion. The characteristic scale related to this transition can be read off from demanding $z_t \sim 1$, and reads $\omega_c = \hat{q}(t)t^2/2$.